Faraday Discussions

Accepted Manuscript

This manuscript will be presented and discussed at a forthcoming Faraday Discussion meeting. All delegates can contribute to the discussion which will be included in the final volume.

Register now to attend! Full details of all upcoming meetings: http://rsc.li/fd-upcoming-meetings

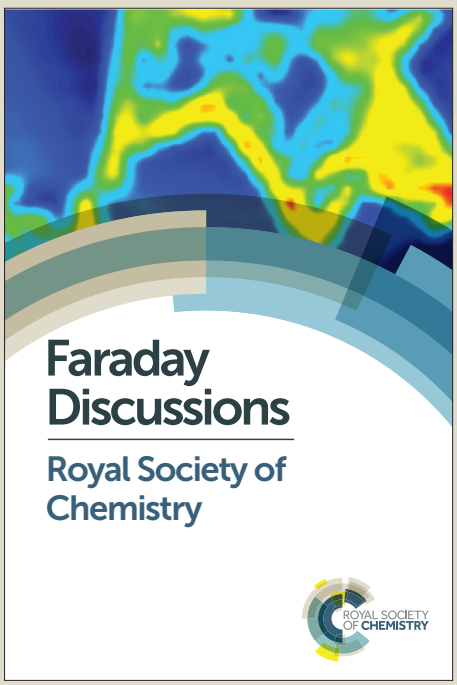

This is an *Accepted Manuscript*, which has been through the Royal Society of Chemistry peer review process and has been accepted for publication.

Accepted Manuscripts are published online shortly after acceptance, before technical editing, formatting and proof reading. Using this free service, authors can make their results available to the community, in citable form, before we publish the edited article. We will replace this *Accepted Manuscript* with the edited and formatted *Advance Article* as soon as it is available.

You can find more information about *Accepted Manuscripts* in the Information for Authors.

Please note that technical editing may introduce minor changes to the text and/or graphics, which may alter content. The journal's standard Terms & Conditions and the Ethical guidelines still apply. In no event shall the Royal Society of Chemistry be held responsible for any errors or omissions in this *Accepted Manuscript* or any consequences arising from the use of any information it contains.

ROYAL SOCIETY OF CHEMISTRY

www.rsc.org/faraday_d

Enhanced Raman Scattering from Aromatic Dithiols Electrosprayed into Plasmonic Nanojunctions

Patrick Z. El-Khoury,[a,] Grant E. Johnson,[a] Irina V. Novikova,[b] Yu Gong,[a] Alan G. Joly,[a] James E. Evans,[b] Mikhail Zamkov,[c] Julia Laskin,[a] and Wayne P. Hess [a,*]*

[a]Physical Sciences Division, Pacific Northwest National Laboratory, Richland, WA 99352, USA; [b]Environmental and Molecular Sciences Laboratory, Pacific Northwest National Laboratory, Richland, WA 99352, USA; [c]Department of Physics and the Center for Photochemical Sciences, Bowling Green State University, Bowling Green, OH 43403, USA

[*]*patrick.elkhoury@pnnl.gov, wayne.hess@pnnl.gov*

ABSTRACT

We describe surface enhanced Raman spectroscopy (SERS) experiments in which molecular coverage is systematically varied from 3.8 x 10^5 to 3.8 x 10^2 to 0.38 molecules/μm^2 using electrospray deposition of ethanolic 4,4'-dimercaptostilbene (DMS) solutions. The plasmonic SERS substrate used herein consists of a well-characterized 2-dimensional (2D) array of silver nanospheres [see El-Khoury *et al.*, *J. Chem. Phys.*, 2014, **141**, 214308], previously shown to feature uniform topography and plasmonic response, as well as intense SERS activity. When compared to their ensemble averaged analogues, the spatially and temporally averaged spectra of a single molecule exhibit several unique features including: (i) distinct relative intensities of the observable Raman-active vibrational states, (ii) more pronounced SERS backgrounds, and (iii) broader Raman lines indicative of faster vibrational dephasing. The first observation may be

understood on the basis of an intuitive physical picture in which removal of averaging over multiple molecules exposes the tensorial nature of Raman scattering. When an oriented single molecule gives rise to the recorded SERS spectra, the relative orientation of the molecule with respect to vector components of the local electric field determines the relative intensities of the observable vibrational states. Using a single molecule SERS framework described herein, we derive a unique molecular orientation in which a single DMS molecule is isolated at a nanojunction formed between two silver nanospheres in the 2D array. The DMS molecule is found lying nearly flat with respect to the metal. The derived orientation of a single molecule at a plasmonic nanojunction is consistent with observations (ii) and (iii). In particular, a careful inspection of the temporal spectral variations along the recorded single molecule SERS time sequences reveals that the time-averaged SERS backgrounds arise from individual molecular events, marked by broadened SERS signatures. We assign the broadened spectra along the SERS time sequence – which sum up to a SERS background in the averaged spectra – to instances in which the π-framework of the DMS molecule is parallel to the metal at a classical plasmonic nanojunction. This also accounts for Raman line broadening as a result of fast vibrational dephasing, and driven by molecular reorientation at a plasmonic nanojunction. Furthermore, we report on the molecular orientation dependence of single molecule SERS enhancement factors. We find that in the case of a single DMS molecule isolated at a plasmonic nanojunction, molecular orientation may affect the derived single molecule SERS enhancement factor by up to 5 orders of magnitude. Taking both chemical effects as well as molecular orientation into account, we were able to estimate a single molecule enhancement factor of ~10^{10} in our measurements.

1. Introduction

The dynamic coupling between molecular polarizabilities and electric fields leads to Raman scattering. Surface-enhanced Raman scattering (SERS)[1,2,3,4] is a variant of Raman scattering in which the driving fields are typically light waves trapped at the surface of metal nanostructures in the form of localized surface plasmons. The effect is particularly evident in assemblies of plasmonic nanostructures, where the plasmonic Eigenmodes of individual particles hybridize to form new collective modes in the assembly.[5,6,7] Confined and enhanced local electric fields at plasmonic nanojunctions formed between interacting plasmonic particles rendered SERS particularly popular, ever since the possibility of single molecule detection sensitivity in such constructs was demonstrated.[8,9] The single/few molecular SERS regime is slowly becoming routinely accessible through the use of engineered plasmonic substrates, as highlighted in recent reviews.[10,11] In this contribution, we examine the information content in Raman scattering from aromatic dithiols, namely 4,4'-dimercaptostilbene (DMS) molecules, addressed at well-defined plasmonic nanojunctions.

Pioneering SERS works were based on the low-concentration approach to explore the single molecule SERS realm.[8,9] Namely, the samples used therein featured 1 (or less) molecular scatterer per effective SERS probing volume, defined by a high numerical aperture microscope objective. The ultra-low concentration approach was challenged over the years, particularly for colloidal solutions, where several convoluted factors come into play in the interpretation of fluctuating Raman spectra.[10] Besides obvious considerations such as the number of plasmonic particles/unit volume, shape and polydispersity of the particles, and physisorption or chemisorption efficiency of the molecular reporters onto the particles,[10] the major challenge lies in our inability to precisely control or even directly characterize molecules and plasmonic

constructs over the relevant length scales (sub- to a few- nm) in solution. Even in the case of solid or dried plasmonic substrates well-characterized using high-resolution microscopic techniques such as transmission electron microscopy (TEM), typical sample preparation methods introduce further challenges. Namely, SERS samples are conventionally prepared by (i) mixing plasmonic particles with dilute solutions of SERS analytes, (ii) drop/spin casting dilute analyte solutions onto solid/dried plasmonic substrates, or (iii) incubating plasmonic substrates in dilute analyte solutions and allowing time for adsorption/chemisorption to take place. In all (i)-(iii), the exact location and number of probed molecule(s) in the effective SERS sampling area vary for different plasmonic substrates/molecular SERS reporters and are overall ill-determined. For instance, factors such as preferable adsorption/chemisorption of analytes at specific sites of metal substrates are not easily discernible. In this regard, isolated engineered prototypical dumbbell antennae, defined by an aromatic dithiol at the junction formed between two plasmonic nanospheres and prepared through (i) are more telling.[12,13] Indeed, such constructs have been recently used to explore some of the underlying physics in single molecule SERS based on strong relative intensity and background fluctuations in Raman spectral sequences, *vide infra*.

Although much evidence supports it, the inference of single molecule sensitivity in ambient SERS is not trivial. The origin of intensity fluctuations in few/single molecule SERS in sequentially recorded SERS (and tip-enhanced Raman scattering, TERS) spectra is still a subject of debate, four decades after the first observation of SERS.[13,14] Even the original observation[9] of quantized probability distributions corresponding to 0, 1, 2, and 3 molecules in the SERS probing volume was later challenged on the basis of insufficient statistical sampling.[10] More recent works[13,15,16] have associated mode-specific intensity variations in non-resonant SERS and TERS with molecular reorientation at plasmonic nanojunctions. Namely, the removal of

orientational averaging in the single molecule regime exposes the tensorial nature of Raman scattering. As such, relative intensity fluctuations may be used to track the orientation of single molecules relative to the local electric fields.[13,15,16] In this context, the use of non-resonant reporters in SERS and TERS turns into a comparative advantage, as technical (photobleaching, photochemistry, resonant heating, etc.) and theoretical challenges[14] arise in interpreting surface- and tip-enhanced *resonant* Raman scattering. In the following, we will provide a brief overview of our recent SERS and TERS studies, focused at understanding the origins of inelastic light scattering from aromatic dithiols at plasmonic nanojunctions. The brief summary justifies and leads into the strategy adopted herein to achieve and demonstrate single molecule detection sensitivity in Raman scattering from aromatic dithiols at plasmonic junctions.

In a series of recent reports from our group, we examined the information content in SERS and TERS point spectra[16,17,18] and images[19,20] recorded by taking advantage of light confinement at plasmonic junctions, all using DMS and a structurally related biphenyl-4,4'-dithiol (BPDT) system as prototypical molecular reporters. We distinguished between two regimes encountered in TERS of the two dithiols, where plasmonic junctions are formed between the metal AFM tip and a metal surface.[16-20] In contact mode TERS experiments, in which a plasmonic junction is formed between a metal AFM tip *in contact* with a metal surface coated with dithiols,[17,18] we identified optical signatures[13] of current carrying charge-transfer plasmons. Indeed, a recent quantum analysis of plasmonic junctions[21] suggests that in the case of strongly coupled plasmonic particles (0-1 nm particle separation), conductive overlap is established. The onset of electron tunneling is accompanied by broadened Raman scattered signals in which only molecular parentage is apparent.[13,17,18] In contrast, *non-contact* mode TERS experiments in which the AFM probe oscillates atop the dithiol-coated metal substrate resulted in familiar tip-

enhanced molecular line spectra.[16,19] Relative intensity fluctuations in sequences of *non-contact* mode TERS spectra were evident, and were associated with molecular reorientation at plasmonic nanojunctions.[16,19] Notably, the effect was recognizable in TERS point spectra[16] and also governed nanoscale chemical images recorded using the same technique.[19,20] Overall, the interplay between molecules and plasmons is evident in SERS and TERS experiments conducted both at the classical and quantum regimes of plasmons. Nonetheless, the transition to the quantum realm of current-carrying plasmons renders structural/chemical selectivity based on single/few molecule SERS and TERS rather difficult to obtain. This is a result of significant broadening of the DMS and BPDT spectra as a result of charge shuttling across the plasmonic gap.[13,17,18]

With the above consideration in mind, we recently designed a sensitive and well-characterized SERS substrate that exclusively operates in the classical regime of plasmons, where the enhancement of recognizable molecular line spectra is optimal.[22] It consists of a self-assembled 2D array of Ag nanospheres with an average particle diameter/inter-particle separation distance of 9/3.7 nm. The structures of the individual particles and their assemblies were characterized using TEM.[22] The plasmonic response of the nanoparticle network was probed using two-photon photoemission electron microscopy (TP-PEEM) and SERS.[22] TEM and TP-PEEM statistics revealed the structure and plasmonic response of the network to be fairly homogeneous on a length scale of tens of microns. This translated into a uniform SERS response from BPDT molecules adsorbed onto different sites of the nanoparticle network. Finite-difference time-domain (FDTD) simulations additionally revealed that plasmonic enhancement factors on the order of 10^6 are attainable at the nanogaps formed between the Ag nanospheres in the 2D array.[22] Combined with modest chemical enhancement factors attainable to aromatic

dithiols at plasmonic nanojunctions,[12,13] this substrate is potentially capable of broadcasting the Raman signature of a single molecule.

In this work, we use the aforementioned SERS substrate.[22] For the above-mentioned reasons, we do not rely on mixing, spin/drop casting, or incubation to functionalize the plasmonic substrate with DMS molecules. Rather, we deposit DMS molecules over the 2D array of silver nanospheres using *ambient* electrospray deposition (ESD).[23,24,25] We find that ESD produces a uniform distribution of intact DMS molecules and allows for superior control over the number of molecules within the effective SERS probing area. This is ideal for this proof-of-principle study in which coverages ranging from a single molecule to molecular ensembles are systematically prepared and probed using SERS. At the smallest coverage tested herein (0.38 molecules/μm^2), we identify and analyze characteristic spectral signatures of SERS at the single molecule limit. Removal of orientational averaging exposes the tensorial nature of single molecule Raman scattering.[16-20,22] The measured relative intensities of the observable vibrational states at the single molecule limit are distinct from their analogues that were recorded from molecular ensembles. This feature allows us to identify an average orientation of a single molecule with respect to the local electric fields defined by a plane polarized laser field incident onto the 2D array of silver nanospheres. The derived 3D orientation of a single DMS molecule at a classical plasmonic nanojunction accounts for our observations of time-fluctuating SERS backgrounds along sequentially recorded SERS spectra. The backgrounds observed in the spatially and temporally averaged spectra recorded at classical plasmonic nanojunctions are associated with individual events: instances along SERS spectral sequences in which a DMS molecule is flat with respect to the metal. This only requires a 30^o rotation around the long axis of a DMS molecule from its derived initial orientation. The derived atomistic picture also

accounts for our observation of broadened Raman lines at lower molecular coverage. The observed SERS line broadening at the single molecule limit is associated with rapid dephasing of molecular vibrations when the π-framework of DMS strongly interacts with the metal surface. We end our analysis by providing an estimate of the recorded single molecule SERS enhancement factor both with and without taking molecular orientation into account. We find that for a DMS molecule isolated at a plasmonic nanojunction, molecular orientation may affect estimations of single molecule SERS enhancement factors by up to five orders of magnitudes.

2. Experimental Methods

2.1 Ambient ESD

A 0.1 mM solution of DMS (Sigma-Alrich) in ethanol (Gold Shield, 200 proof) was successively diluted to 1 μM, 1 nM, and 1 pM aliquots. For ambient ESD experiments, samples were injected through a pulled fused silica capillary (~75 μm inner diameter) tip at a flow rate of 50 μL/hour. A 1 mL glass syringe (Hamilton) mounted on a microprocessor-controlled syringe pump (KD Scientific) was used to feed the electrospray capillary. Samples were prepared in increasing order of concentration to avoid cross-contamination. Ample amounts of pure solvent (and target sample solutions) were also used to clean the syringe and capillary between successive sample preparations. After 1 hour of deposition (50 μL total volume) using a positive ionization mode (4 kV), an area (> 1 cm diameter) of adsorbed species was faintly visible at the surface of the electrically grounded SERS substrates, described below. As such, we estimate upper limits of coverage produced by ESD as 3.8 x10^5, 3.8 x10^2, and 0.38 molecules/μm^2 for the samples prepared using 1 μM, 1 nM, and 1 pM solutions, respectively.

2.2 SERS Substrate

Control experiments were performed by either ESD or drop casting a 0.1 mM solution of DMS in ethanol onto a 15 nm polycrystalline Ag film evaporated on a 0.1 mm-thick microscope glass slide by arc-discharge physical vapor deposition (Cressington 208HR, target: Ted Pella Inc., 99.99% purity). The film thickness was monitored *in-situ* using a quartz crystal microbalance, and the surface roughness measured from freshly evaporated Ag films with AFM indicates a root-mean-square (RMS) height distribution of ~3 nm.[15-17]

Concentration-dependent SERS measurements were performed using a recently reported[22] and thoroughly characterized SERS substrate comprising a 2D array of Ag nanospheres atop a sputtered silver substrate, as described above. In the following, we provide a brief description of previous observations that are of particular relevance to this investigation. The reader is referred to the original work[22] for more specifics. The UV-Vis absorption profile of the synthesized colloidal Ag nanoparticles in chloroform exhibited a sharp plasmon resonance centered at 415 nm, indicative of a narrow size distribution of oleylamine-capped nanoparticles. TEM images corroborated the UV-Vis observables, revealing a relatively narrow size distribution of nearly spherical Ag nanoparticles, featuring an average diameter of 9 ± 2 nm. The recorded TEM images also revealed that drop casting the as-synthesized nanoparticle solution yielded patches of uniformly self-assembled 2D Ag nanoparticle networks. They are best described as hexagonal close packed distributions of Ag nanospheres with an average inter-particle separation distance of 3.7 nm in the network. The plasmonic properties of the assemblies were probed using TP-PEEM. Oversampled TP-PEEM image statistics revealed the plasmonic response of the network to be homogeneous, namely, 90% of the recorded enhancement factors were within a factor of 4 $\left(\left(\frac{E}{E_0}\right)^4\right)$ from the average. The homogeneity in structure and plasmonic response over a length scale of tens of microns gauged from TEM and TP-PEEM analysis

translated into a uniform SERS response from BPDT molecules adsorbed onto different sites of the network from a 0.1 mM ethanolic solution. Finally, FDTD simulations revealed that plasmonic enhancement factors on the order of 10^6 are attainable at the nanogaps formed between the Ag nanospheres in the array following in-plane-polarized irradiation at 514 nm.

2.3 SERS Experiments

SERS measurements were conducted using an inverted optical microscope (Axiovert 200, Zeiss). The incident 514 nm continuous wave laser light (Innova 300, Coherent) is attenuated using a variable neutral density filter wheel (150-300 $\mu W/\mu m^2$ used throughout), reflected off a dichroic beamsplitter, and focused onto the sample surface using an oil-immersion objective (1.3 NA, 100 X). The diameter of the diffraction limited laser spot was measured to be 260 nm using non-contact mode TERS imaging of a DMS coated thin Ag film.[19] As such, our effective SERS probing area is 0.053 μm^2.The polarization of the incident laser is controlled using a half wave plate, which allows polarization rotation in the sample plane. The polarization of the incident laser field was readjusted prior to recording each of the spectral sequences reported herein, such that the molecular signal at 1575 cm^{-1} was maximized. No polarizers were used to analyze the backscattered radiation, which is collected through the same objective, transmitted though the dichroic beamsplitter, and filtered through a long pass filter. The resulting light is detected using a liquid nitrogen cooled charge coupled device (CCD) coupled to a spectrometer (Holespec f/1.8i, Kaiser Optical System). The effective instrument spectral resolution in the micro-Raman experiments is 8 cm^{-1}.

2.4 Theoretical Framework

Calculations were performed using methodologies implemented in Gaussian 09,[26] and employed the B3LYP[27,28,29,30] exchange-correlation functional in conjunction with the 6-311^{++}G**[31,32] basis set. Unconstrained geometry optimization was performed to energy minimize the structure of DMS in its ground electronic state. Frequency-dependent molecular polarizability derivative tensors were computed using the Raman optical activity[33,34] module of Gaussian 09 at an incident wavelength of 514 nm. Standard Euler-averaged Raman scattering activities were evaluated near the ground state minimum according to

$$S_n = 45\bar{\alpha}_n'^2 + 7\gamma'^2_n \qquad (1)$$

in which $\bar{\alpha}_n'$ and γ'^2_n are the spherical and anisotropic parts of the molecular polarizability derivative tensors given by

$$\bar{\alpha}_n' = \frac{1}{3}\left(\frac{\partial\alpha_{xx}}{\partial Q_n} + \frac{\partial\alpha_{yy}}{\partial Q_n} + \frac{\partial\alpha_{zz}}{\partial Q_n}\right) \qquad (2)$$

$$\gamma'^2_n = \frac{1}{2}\left(\frac{\partial\alpha_{xx}}{\partial Q_n} - \frac{\partial\alpha_{yy}}{\partial Q_n}\right)^2 + \frac{1}{2}\left(\frac{\partial\alpha_{yy}}{\partial Q_n} - \frac{\partial\alpha_{zz}}{\partial Q_n}\right)^2 + \frac{1}{2}\left(\frac{\partial\alpha_{zz}}{\partial Q_n} - \frac{\partial\alpha_{xx}}{\partial Q_n}\right)^2 + 3\left(\frac{\partial\alpha_{xy}}{\partial Q_n}\right)^2 + 3\left(\frac{\partial\alpha_{yz}}{\partial Q_n}\right)^2 + 3\left(\frac{\partial\alpha_{zx}}{\partial Q_n}\right)^2 \qquad (3)$$

where α_{ij} are diagonal ($i = j$) and off-diagonal ($i \neq j$) molecular polarizability derivative tensor elements and Q_n are the coordinates for the n^{th} vibrational mode. To ease spectral assignments, we also performed a full anharmonic vibrational frequency analysis based on perturbation correction for the harmonic approximation.[35] The resulting theoretical Raman spectra are thus compared to their experimental analogues without applying any scaling factors. Throughout the text, the computed spectra are represented as a sum of Lorentzians individually broadened by 8 cm^{-1} to match our effective instrument resolution, and centered at the calculated anharmonic

frequency shifts. To compare the computed Raman scattering activities with experimental intensities, a useful quantity is the differential Raman scattering cross section, $\frac{d\sigma}{d\Omega}$, defined in terms of S_n as

$$\frac{d\sigma}{d\Omega} = \frac{(2\pi)^4}{45}\frac{h\omega_s^4}{8\pi^2 c\omega_n}\frac{S_n}{1-e^{-\left(\frac{hc\omega_n}{k_b T}\right)}} \qquad (4)$$

in which ω_s is the scattered frequency in cm^{-1}, ω_n is the frequency of the n^{th} vibrational mode in cm^{-1}, and the calculated S_i is typically in $A^4\ amu^{-1}$, governed by equations (1-3).

In the realm of a single/few molecules, orientational averaging according to equations (1-3) is no longer appropriate.[13,15,16,19] In this case, the scattering tensor that governs Raman activity may be expressed as

$$S_n^2 = \sum_n \left| E_s^L \alpha_n'(\Omega) E_i^L \right|^2 \qquad (5)$$

where $E_{i,s}^L$ are the enhanced incident and scattered local electric fields, α_n' is the molecular polarizability derivative tensor of the n^{th} vibrational Eigenstate, and $\Omega = \{\alpha, \beta, \gamma\}$ are the Euler angles which determine molecular orientation relative to the local fields. This formalism stresses that a single molecule assumes a unique orientation with respect to the local electric fields. As such, the observable relative intensities in single molecule SERS may be used to track the orientation of a molecule in 3D where $E_{i,s}^L$ are known, e.g. at a hot spot formed between two interacting plasmonic particles.[12,13] Alternatively, if molecular orientation is known, the vector components of the local electric field may be inferred from the relative intensities in single molecule SERS spectra. If neither molecular orientation nor local electric fields are known, removal of orientational averaging according to equation (5) yields a unique set of relative

intensities for every orientation of a molecule with respect to the local fields. This framework was recently used to track reorientation dynamics of molecules at plasmonic junctions in SERS and TERS experiments.[13,16,19] Overall, it provides an intuitive framework that may be used to rationalize observables such as relative intensity fluctuations in the single molecule realm. Its limitations have been noted elsewhere,[36,37] and will be further stressed in context.

3. Results and Discussion

3.1 Control Experiments: Sputtered Silver Film on Glass

We begin our analysis by comparing SERS spectra recorded from two samples prepared either by ESD or drop casting a 0.1 mM solution of DMS in ethanol onto freshly sputtered Ag films on glass. The results are illustrated in Figure 1, in which panels A (drop casted) and C (ESD) show several spectra recorded from randomly selected spots separated by tens of microns on the metal surface. We note that each of the spectra shown in the aforementioned two panels represents a time average of 60 consecutively collected spectra that were individually integrated for 10 s at one position. The spatially and temporally averaged spectra in the two cases are expanded and shown in panels B (drop casted) and D (ESD) of the same figure, along with their corresponding standard deviations. It is immediately noticeable that the percent deviation from the average spectrum is twice narrower for the sample prepared using ESD. The substrate coated using ESD features a more spatially uniform DMS distribution. Nonetheless, the spectral features in the 500-1700 cm^{-1} region of the spectrum are very similar in the two cases. This is more obvious in Figure 2A, where the two spatially and temporally averaged spectra are normalized and compared on the same plot. Apart from minor background differences in the 500-800 cm^{-1}

region, no noticeable differences are observed between the two experimental spectra both in terms of frequency shifts and relative intensities. These control experiments reveal that ESD yields a uniform distribution of molecules for SERS analysis, all while preserving the chemical identity of the molecules. Moreover, given a total volume of 50 μL deposited in an area of ~0.79 cm^2 (1 cm diameter, lower limit), an upper limit of 3.8 $x10^7$ molecules/μm^2 may be estimated. This value assumes that (i) 100% transfer of molecules from the 0.1 mM DMS solution to the Ag substrate, and (ii) all the molecules are packed in a circular cross-section with a diameter of 1 cm.

The theoretical orientationally averaged B3LYP/6-311^{++}G** Raman spectrum, computed according to equations (1-3) is also shown in Figure 2A, for comparison. We find that the level of theory used herein reproduces the corresponding experimental observables in which molecular ensembles are probed, both in terms of frequency shifts and relative intensities. The latter is an important observation to keep in mind in going through the ensuing theoretical analysis of the samples featuring increasingly sparse molecular distributions.

3.2 Ensemble vs. Single Molecule SERS: 2D Nanosphere Array

The second set of SERS spectra were recorded from three different samples prepared by ESD of 1 μM, 1 nM, and 1 pM solutions of DMS in ethanol. We estimate upper limits of 3.8 $x10^5$, 3.8 $x10^2$, and 0.38 molecules/μm^2 for the samples prepared using 1 μM, 1 nM, and 1 pM solutions, respectively. It is perhaps worth re-iterating that the effective SERS probing area is 0.053 μm^2, that is 19 times smaller than the 1 μm^2 unit area used in our estimation of molecular coverage on the surface of the substrate. The SERS substrate in this set of measurements consists of a 2D array of plasmonic silver nanospheres, see the methods sub-section of this work and our

previous work[22] for more specifics. The results are summarized in Figures 2B-E, where spatially and temporally averaged SERS spectra are compared on the same plot.

Three main observations are highlighted. First, systematically decreasing the number of DMS molecules in the effective SERS probing area leads to a more pronounced SERS background. The background spans the entire spectral region of interest (500-2250 cm^{-1}) and increases in magnitude as a function of decreasing molecular coverage. Second, the relative intensities of the major characteristic molecular Raman lines of DMS, expanded in panels C and E of Figure 2, also exhibit systematic variations as a function of molecular coverage. This is noticeable in Figure 2E, where the ratio of the predominant aromatic C═C stretching (1575 cm^{-1}) to the vinyl C═C stretching (1625 cm^{-1}) vibrations increases with decreasing surface coverage of DMS. A similar trend is observed when the relative scattering activities of the C─S stretching (1085 cm^{-1}) and aromatic C─H in-plane rocking (1186 cm^{-1}) vibrations are compared in Figure 2C. Third, the widths of the observable Raman lines increase as a function of decreasing molecular coverage. The effect is most evident in the 1200-1500 cm^{-1} spectral region shown in Figure 2D, but also noticeable in Figures 2C and 2E. This particular observation is counter-intuitive at first blush, as inhomogeneous broadening would be expected to lead to the opposite trend. In fact, pictures in which contributions from individual molecules with slightly different resonances sum up to an overall broad line shape typical of the ensemble are often invoked in this context. We will illustrate why the aforementioned spectral analysis may lead to erroneous conclusions in the interpretation of single molecule *vs.* ensemble-averaged spectra, at least in our case of Raman scattering of aromatic dithiols at plasmonic nanojunctions. Overall, the key to understanding all three observations is in the analysis of the spatial and temporal variations in

Raman scattering activities, both of which are masked in the spatially and temporally averaged spectra discussed thus far.

3.3 Spectral Fluctuations in Single Molecule SERS

Time-averaged SERS spectra recorded at randomly selected spots on three substrates prepared by ESD of 1 μM (panel A), 1 nM (panel C), and 1 pM (panel E) DMS solutions in ethanol are presented in Figure 3. Variations in the magnitudes of the recorded SERS backgrounds are most evident in panel E, i.e. in the single molecule regime. Less pronounced SERS background variations are still observable in the hundreds-of-molecules regime (panel C), but are negligible at higher molecular coverage (panel A). Our primary analysis of the temporal variations in SERS activity at select spots on each sample is also shown in the same figure (panels B, D, and F). Namely, shown are time averaged spectra at one spot for each of the three DMS coverages along with their corresponding standard deviations derived from sequences of 60 consecutively recorded spectra, each of which was individually integrated for 10 s. The standard deviation error bars again show that ensemble averaged SERS spectra (panel B) exhibit much less pronounced background fluctuations when compared to their analogues that were recorded from samples featuring lower molecular coverages of DMS (panels D and F). Before examining the nature of the fluctuating background further, we note that the relative intensities of the predominant Raman-allowed vibrational states are very similar when the time-averaged spectra recorded at different positions of the substrate and at the same molecular coverage are compared to one another. This is to be expected at high molecular coverage (panel A): the response is orientationally averaged. At low molecular coverage (panel E), this observation is indicative of similar local environments felt by the different (individual) molecules probed. Given a uniform SERS substrate, and subsequently a uniform plasmonic response,[22] this

observation suggests that similar molecular orientations are assumed at the various plasmonic nanojunctions probed in this work.

To better illustrate the nature of the fluctuating backgrounds we now turn the reader's attention to Figure 4, where representative spectra along the SERS time sequences are shown. Sequentially recorded spectra (Δt =10 s) are plotted in panels A and B, where subtle background fluctuations are observable in the hundreds-of-molecules regime, and dominate the SERS response in the single molecule regime. As the background fluctuations in Figure 4B mask more subtle relative intensity fluctuations, we select another spectral sequence in which the SERS background is relatively stable over time for further analysis. In this particular time sequence, frequency slices taken at select molecular resonances are shown in panel C, and sequentially recorded spectra (10 s/spectrum) along the representative time sequence are shown in panel D. It is shown in panel C that the different molecular resonances exhibit distinct time evolution trends along the SERS trajectory. This is evident, for example, around spectrum 30 (t = 300 s, highlighted with a transparent light blue rectangle) where an intensity spike at 1575 cm^{-1} is not evident in the 1186 and 1085 cm^{-1} time traces. In Panel D, the most obvious intensity fluctuations along the time sequence are observed in the 500-1000 cm^{-1} region of the spectrum, in which the appearance/disappearance of at least three distinct vibrational signatures may be readily discerned. More subtle relative intensity fluctuations are also observable in the 1250-1500 cm^{-1} region of the spectrum. Relative intensity fluctuations in SERS and TERS at plasmonic junctions in the single molecule regime have been recently associated with molecular reorientation dynamics according to equation (5). In principle, the same analysis carried out in the previous works[13,15,16,19] may be performed to extract a unique relative orientation of the molecule with respect to local electric fields for each of the spectra along the time trajectory. We

refrain from duplicating the prior analyses, to which the reader is referred. Rather, we will focus our analysis on identifying the most likely time-averaged molecular orientation of DMS throughout the entire SERS spectral sequence shown in Figure 4C-D, to illustrate the concept.

3.4 Removal of Averaging: Orientation-Specific Single Molecule SERS

In Figure 5, we time-average the SERS sequences shown in Figure 4C-D. Notice how the relative intensities of the observable vibrational states are distinct from the ensemble averaged SERS spectra shown in Figures 1 and 2. Namely, (i) the vinyl C═C stretching vibration (1625 cm^{-1}) is suppressed, (ii) the C─S stretching vibration (1085 cm^{-1}) is more pronounced than the aromatic C─H in-plane rocking (1186 cm^{-1}), and (iii) the vibrational modes in the 1200-1500 cm^{-1} region are heavily broadened and largely buried in the underlying background. On the basis of (i) our SERS-active substrate preparation method of choice (ESD) which yields an upper limit of 0.02 molecules (on average) in our effective SERS probing area, and (ii) the distinct relative intensity patterns observed in the different spectra recorded at low molecular coverage,

we will attribute the observed spectrum to the Raman signature of a single DMS molecule. More evidence in support of this assignment will follow. Using the molecular polarizability derivative tensors derived from B3LYP/6-$311^{++}G^{**}$ calculations, we identify a unique average orientation of a single molecule with respect to vector components of the local electric fields according to equation (5). This is first done in the molecular frame by fixing the molecule and rotating the incident and scattered electric fields until a satisfactory match is found.[13,16] Projecting into the laboratory frame, defined in the inset of Figure 5, and recognizing that the local electric fields are unidirectional (in the x-direction defined in Figure 5), we obtain an average orientation in which the molecule is nearly flat with respect to the surface of the Ag spheres defining the

nanojunction. Specifically, the long axis of the molecule is oriented along the z-axis of the laboratory frame, and the molecule's π-framework is rotated by 32^{o} with respect to the zy plane of the same frame. That the field is unidirectional may be rationalized on the basis of our substrate and experimental geometry. Namely, given a laser source polarized in the sample plane (inverted optical microscopy setup), the inter-particle regions are the only regions in which the local electric fields are maximally enhanced such that the optical signature of a single molecule is detectable.[22] Note that assuming xz-plane polarized laser irradiation to excite the plasmonic junction defined by a molecule positioned between two particles aligned along xz (see the inset of Figure 5) would yield the same relative orientation of the molecule in the corresponding plasmonic junction. As illustrated in Figure 5, the simulated Raman spectrum of the oriented single molecule matches the intensity pattern observed experimentally reasonably well. Overall, we employ 3N-6 (the number of vibrational degrees of freedom) equations to solve for molecular orientation relative to the vector components of the incident/scattered local fields; the derived mathematical solution is rigorous. That said, there are limitations to the framework used herein,[13,36,37] mostly stemming from the approximations invoked in the level of theory employed to compute the molecular polarizability derivative tensors. Those include assuming (i) separable polarizabilies of the molecule and metallic systems, (ii) that the molecular polarizabilities which govern Raman scattering activities are invariant to molecular orientation with respect to the metal substrate, and (iii) truncation at the dipole limit[13] in the expansion of molecular polarizability. These approximations may prove inadequate in many cases, three of which have been noted in recent reports.[13,36,37] Nonetheless, the molecular orientation derived from our analysis accounts for many of the experimental observables described thus far, as discussed below.

3.5 Spectral Fluctuations, Background Fluctuations, and Line Broadening

The main observations in SERS from 3.8 x 10^5, 3.8 x 10^2, and 0.38 DMS molecules/μm^2 adsorbed on a 2D Ag nanosphere assembly are now reiterated, and an expanded interpretation of our experimental observables is provided. The relative intensities of the observable vibrational Eigenstates in the single molecule regime are distinct from their analogues that were recorded from the molecular ensembles. When compared to ensemble average measurement, hundreds of spectra recorded from different regions of the substrate containing only a few DMS molecules per probing area exhibit similar trends: (i) an increased ratio of the predominant aromatic C═C stretching (1575 cm^{-1}) to the vinyl C═C stretching (1625 cm^{-1}) vibrations, and (ii) an increased ratio of the C─S stretching (1085 cm^{-1}) to the aromatic C─H in-plane rocking (1186 cm^{-1}) vibrations. The recorded intensity patterns may be uniquely reproduced according to equation (5). The picture painted through this analysis necessitates that the DMS molecule resides at a nanojunction defined by two silver nanoparticles in the array and is lying nearly flat at the plasmonic nanojunction.

Decreasing the number of molecules in the SERS probing area leads to a larger SERS background. These backgrounds are individual events captured along sequentially recorded SERS spectra, and representative sequentially recorded spectra are shown in Figure 4A-B. Such events are most noticeable at a coverage of 0.38 molecules/μm^2, obscured but still observable at 3.8 x10^2 molecules/μm^2, and mostly averaged out at higher molecular coverage. Individual background fluctuation events sum up to comprise the overall background observed in the temporally averaged spectra. We associate the background-like SERS spectra along the SERS sequences to instances in which the π-framework of the DMS molecule is parallel to the metal surface. Given the average molecular orientation derived from the relative intensities in the

single molecule regime, this only requires a 32° rotation around the z axis of the laboratory frame, see Figure 5. Similar broadened Raman signals have been previously observed in SERS from flat adsorbates, a classical example of which is the SERS spectrum of benzene on Au.[38] They are thought to arise from aromatic ring-metal surface electron density overlap.[39] We similarly associate the intermittent broadened molecular spectra with instances at which the π-framework of DMS is flat with respect to the metal. Rapid dephasing of the vibrational transitions induced by transient flat adsorption events would also explain our observation of broadened Raman lines, see Figure 2C-E. A closer inspection of Figure 5 also reveals that in the 1200-1500 cm^{-1} spectral region, at least 5 predicted vibrational transitions appear as broadened transitions atop the averaged background which spans the entire frequency range. In this context, it appears that homogeneous broadening governs the observable line shapes in junction plasmon-enhanced SERS in the single molecule limit. To comment on why some modes are more rapidly dephased than others would require a more extensive mode-specific theoretical analysis, a challenge we will take up in future works.

3.6 Single Molecule SERS Enhancement Factor

Using the signal derived from the spectrum shown in Figure 5, we may estimate a SERS enhancement factor (EF) according to[13,39]

$$I = EF\, I_0\, \eta_{max}\, \frac{\partial \sigma}{\partial \Omega}\, d\Omega = 390\ s^{-1} \quad (6)$$

Based on a count rate of 390 s^{-1} obtained by integrating over the 1575 cm^{-1} band, an incident intensity of I_0 = 7.76 x 10^{22} photons cm^{-2} s^{-1} (300 μW μm^{-2}), an upper limit for detection efficiency η_{max} = 0.1, a Raman scattering cross-section $\frac{\partial \sigma}{\partial \Omega}$ = 7.47 x 10^{-28} cm^2 sr^{-1} (calculated

according to Equation (4) for an incident laser wavelength of 514 nm, $S_{1575\ cm^{-1}}$ = 11818 A^4 amu^{-1}), and a solid angle $d\Omega = \pi$, we derive an enhancement factor of 2.1 x 10^6 for the bright aromatic C=C stretching vibration at 1575 cm^{-1}. A plasmonic enhancement factor on the order of 10^6 is certainly attainable at the plasmonic nanojunctions within the 2D Ag nanosphere array-SERS substrate used in this work.[22] The largest error in the current estimation arises from the computed $\frac{\partial\sigma}{\partial\Omega}$ value, which (i) does not account for molecular orientation, as $S_{1575\ cm^{-1}}$ is an orientationally averaged quantity (see equations (1-3)), and (ii) is derived from an isolated gas-phase DMS molecule and hence does not account for static and dynamic changes in molecular polarizability as a result of chemisorption/adsorption onto a metallic surface. Although quantitative estimates of both (i) and (ii) are challenging, we will attempt to shed light on both effects by relying on our density functional theory calculations and single molecule framework and experiments.[15,16,19] Given the molecular orientation derived from our single molecule Raman simulation according to equation (5), we find that the largest Raman scattering cross-section for the 1575 cm^{-1} mode is attainable at $E_i^L = E_S^L = (0,0,1)$ in the laboratory frame, see Figure 5. This is expected, given the large polarizability associated with π-conjugated electrons aligned along the z-axis. When $E_i^L = E_S^L = (1,0,0)$, i.e. the same relative orientation used to produce the fit shown in Figure 5, we find that the calculated EF is underestimated by a factor of ~10^5 where the rotationally averaged value of $S_{1575\ cm^{-1}}$ is used to calculate EF based on equation (6). On the other hand, using an $S_{1575\ cm^{-1}}$ value derived from the isolated molecule yields an overestimated EF value, as static and dynamic polarizability changes to the molecule upon chemisorption are expected to render DMS a more efficient Raman scatterer. To account for chemical effects, we consider another model structure in which DMS is chemisorbed onto the vertex of a finite pyramidal Ag_{20} cluster and recalculate $S_{1575\ cm^{-1}}$.[18,19] Here, only a small factor

of 30X increase in Raman scattering activity (30X decrease in EF) is obtained, consistent with a prior analysis of chemical enhancement factors in SERS of aromatic dithiols.[12] Taking both the molecular orientation dependence and chemical effects into account allows us to re-estimate the EF to be ~10^{10}, required to observe 390 counts/s from a single DMS molecule under the above-described experimental conditions. To the best of our knowledge, this is the first report in which molecular orientation is taken into account in estimating SERS enhancement factors.

4. Conclusions

We report SERS from a uniform 2D array of Ag nanospheres coated with increasingly sparse distributions of DMS molecules using ESD. Knowing the concentration and volume of the DMS solutions deposited into an area > 1 cm in diameter, we are able to estimate an upper limit for the number of molecules in our effective SERS probing area. The lowest concentration used featured << 1 molecule per probed area. Systematically decreasing the molecular coverage of DMS resulted in spectral changes: (i) more pronounced SERS background signals at lower concentrations, (ii) increased widths of the observable vibrational lines at lower concentrations, and (iii) systematic changes in the relative intensities of the observable vibrational signatures of DMS. The backgrounds observed in the spatially and temporally averaged SERS spectra are associated with individual events that are particularly evident at pM concentrations, observable but less pronounced at nM concentrations, and less evident at higher molecular coverage. Namely, transient flattening of a DMS molecule at a plasmonic junction leads to a broadened response of molecular origin. Overall, these individual background fluctuations sum up to a SERS background in the time averaged signals. This picture is also consistent with the observed Raman line broadening. In this regard, homogeneous broadening of a molecule interacting with its local environment governs the observable line shapes in junction plasmon-enhanced SERS

from DMS molecules at classical plasmonic junctions. The observation of distinct relative intensities in the low *vs.* high coverage regimes is associated with removal of Euler averaging which exposes the tensorial nature of Raman scattering in the single molecule limit. Using a representative sequence recorded at the single molecule limit, we identify a time averaged orientation of a single DMS molecule at a plasmonic junction formed between two Ag particles in the array. Taking the derived molecular orientation into account allows us to estimate a SERS enhancement factor of up to ~10^{10} in our measurements. Overall, our analysis suggests that molecular orientation is a key factor that needs to be taken into consideration when estimating single molecule SERS enhancement factors. Herein, we find that in the case of a nearly flat-lying π-conjugated molecule, molecular reorientation may affect the derived SERS enhancement factor by about five orders of magnitude.

The inference of single molecule detection sensitivity in this work was not proven with a definite test, e.g. using the bi-analyte approach.[10] Nonetheless, given (i) our SERS-active substrate preparation method of choice (ESD) which yields an upper limit of 0.02 molecules in our effective SERS probing area, (ii) the above-mentioned spectral signatures that can be associated with the removal of orientational averaging, and (iii) a derived single molecule SERS enhancement factor of ~10^{10}, it is likely that all the spectra that were recorded at ultralow molecular coverage are those of single molecules. Our analysis also suggests that time-dependent orientational dynamics which affect the electronic structure of a molecular system chemisorbed/physisorbed onto metal substrates comprise another factor which needs to be considered in an effort to accurately account for single molecule SERS observables. We hope that this contribution fuels future theoretical and experimental works aimed at attaining a

detailed understanding of specific molecule-metal interactions which govern surface-enhanced linear and nonlinear ultrasensitive spectroscopies.

Acknowledgements

WPH, JL, AGJ, YG, and GEJ acknowledge support from the US Department of Energy (DOE), Office of Science, Office of Basic Energy Sciences, Division of Chemical Sciences, Geosciences & Biosciences. PZE acknowledges support from the Laboratory Directed Research and Development Program (LDRD) through a Linus Pauling Fellowship at Pacific Northwest National Laboratory (PNNL), an allocation of computing time from the National Science Foundation (TG-CHE130003), and the use of the Extreme Science and Engineering Discovery Environment. A portion of the work was performed using EMSL, a national scientific user facility sponsored by the DOE's Office of Biological and Environmental Research and located at PNNL. This work also benefitted from PNNL Institutional Computing resources. PNNL is a multiprogram national laboratory operated for DOE by Battelle.

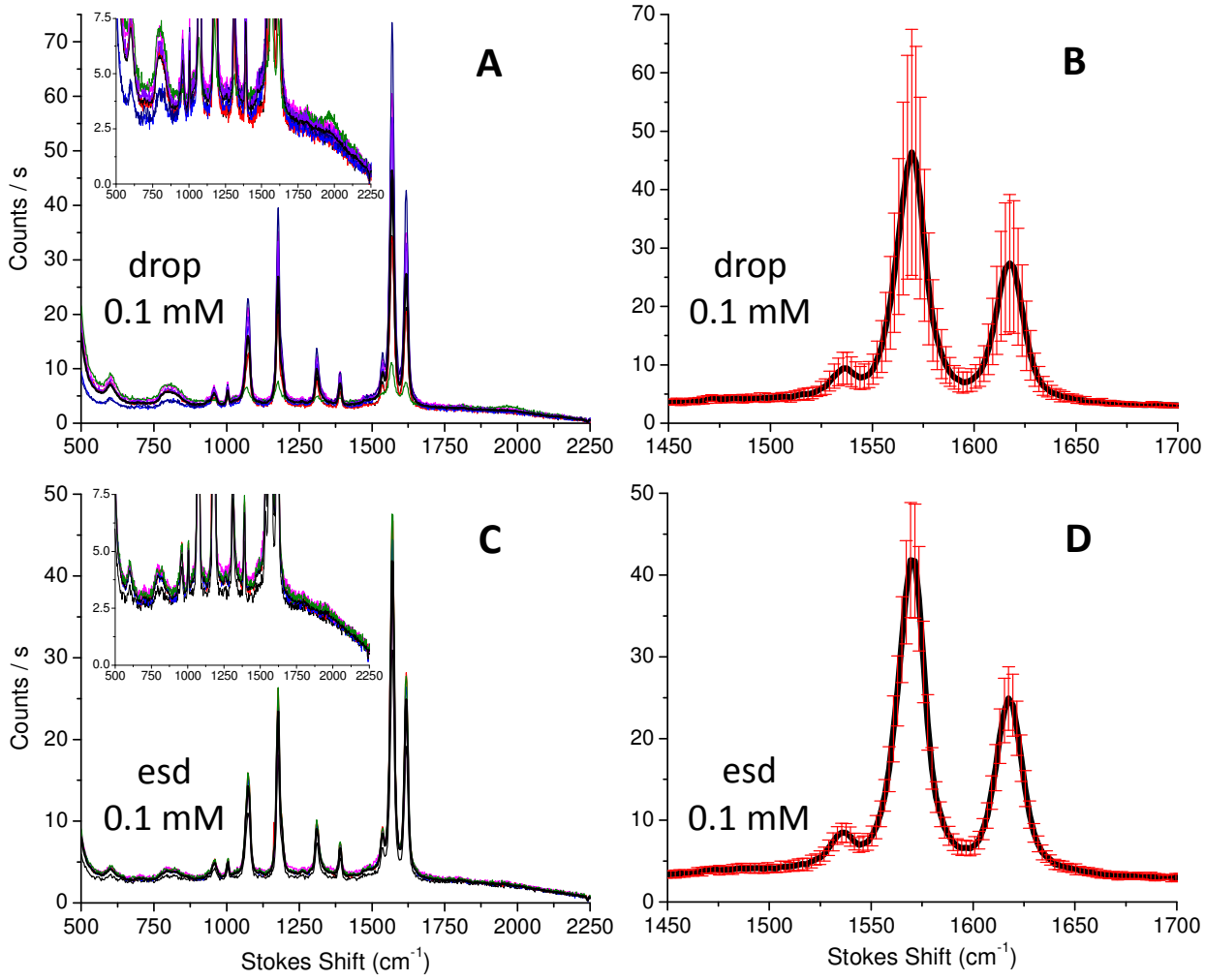

Figure 1. Control experiments: SERS spectra recorded from samples prepared either by drop casting (A-B) or electrospray deposition (C-D) of a 0.1 mM solution of 4,4'-dimertcaptostilbene in ethanol. Shown in panels A and C are several time-averaged spectra recorded from randomly selected spots on a sputtered silver substrate. Shown in Panels B and D are the spatially and temporally averaged spectra for each case (in the 1450-1700 cm^{-1} region) along with the standard deviation of the various spectra shown in panels A and C, respectively.

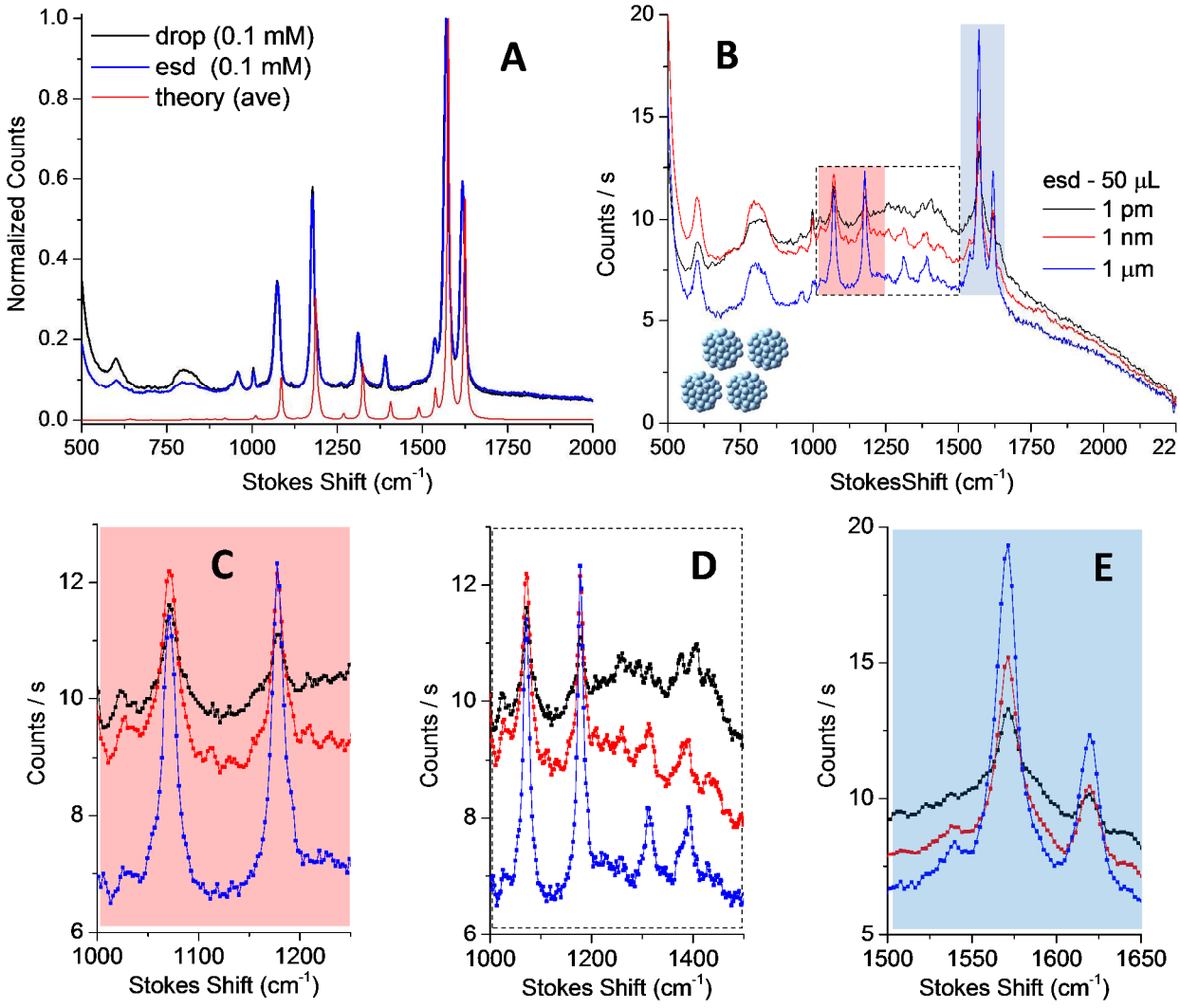

Figure 2. A) The spatially and temporally averaged SERS spectra shown in Figure 1 (control experiments) are shown on the same plot, along with the orientationally averaged Raman spectrum of an isolated DMS molecule calculated at the B3LYP/6-311^{++}G** level of theory. Note that in the computed spectrum, the intensities are obtained from dynamic polarizability calculations (λ_{ex} = 514 nm) and the frequency shifts are obtained after explicit anharmonic frequency corrections including third and fourth derivatives, see text for more details. B) Spatially and temporally averaged SERS spectra recorded from the 2D Ag nanoparticle array at

DMS coverages of 3.8 x10^5 (1 μM), 3.8 x 10^2 (1 nM), 0.38 molecules/μm^2 (1 pM). Three spectral regions of interest are highlighted in panel B, and in turn expanded in panels C-E.

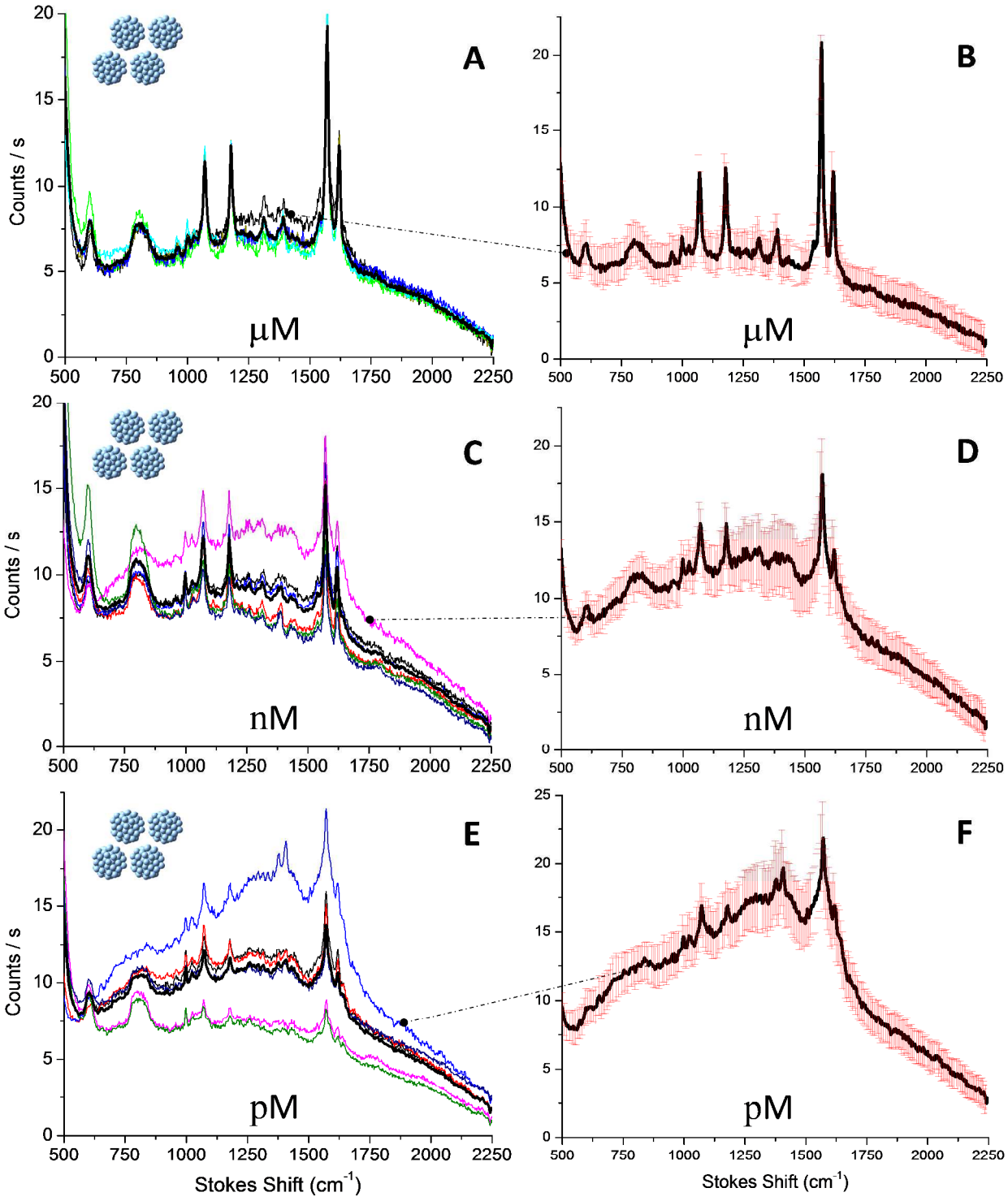

Figure 3. Panels A, C, and E show time-averaged spectra recorded from randomly selected spots on the 2D Ag nanoparticle array at different DMS coverages. Each spectrum shown is an average

of 60 spectra, each of which was time-integrated for 10 s. Panels B, D, and F show 3 temporally averaged spectra along with the standard deviation for the SERS time-sequences that were averaged to yield the selected spectra. The concentrations used in electrospray deposition of DMS solutions are denoted in the insets.

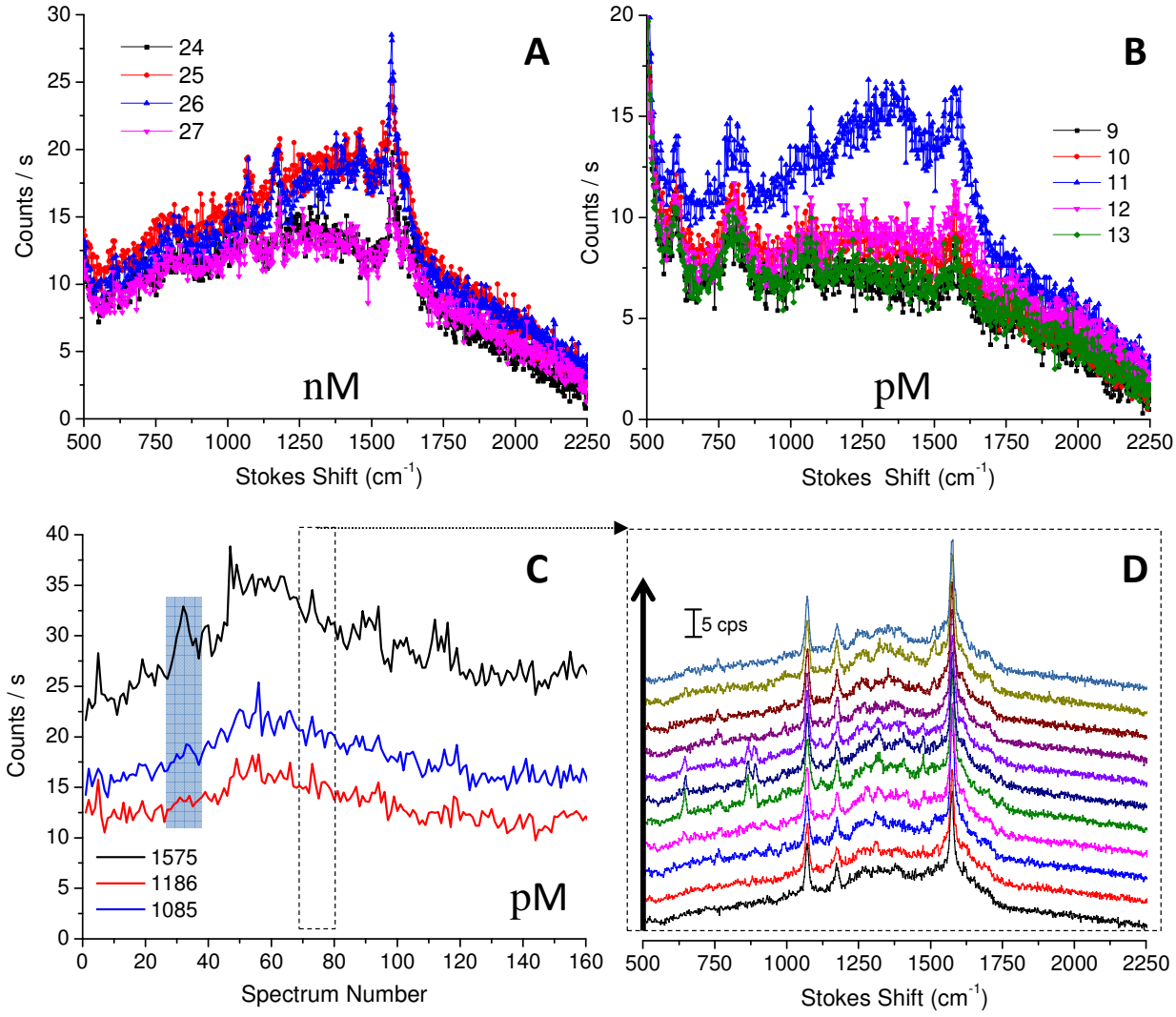

Figure 4. Spectral variations along SERS time sequences at 3.8 x 10^2 DMS molecules/μm^2 (1 nM, panel A) and 0.38 DMS molecules/μm^2 (1 pM, panel B). Note that the spectra shown in panels A and B are selected sequentially recorded SERS spectra along a time-sequence, where each spectrum is individually time-integrated for 10 s. Panels C and D show another selected SERS spectral sequence. In panel C, we monitor the time evolution of SERS intensity at three vibrational resonances of DMS. Two highlighted regions in panel C are noted. The first (transparent blue rectangle) shows distinct relative intensity fluctuations along the SERS time

sequence. The second (dashed rectangle, spectra 70-80) is expanded in panel D, which further illustrates temporal relative intensity fluctuations along the SERS time sequences.

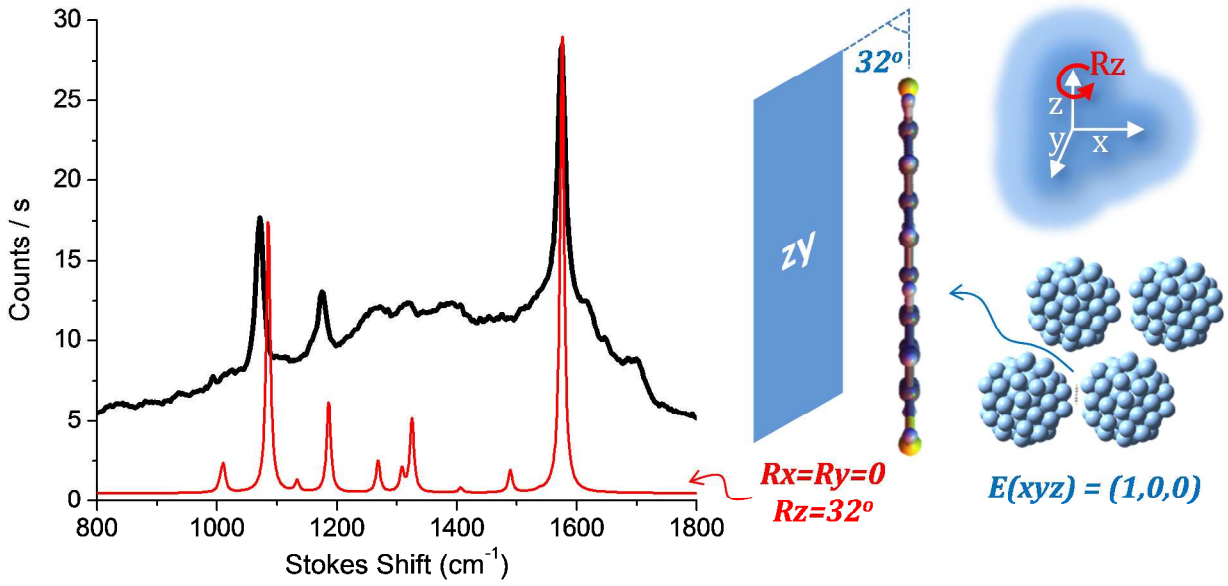

Figure 5. The SERS sequence shown in panels C and D of Figure 4 is time averaged (black trace) and compared to the Raman spectrum of an oriented single DMS molecule (red trace) simulated according to equation (5) in the main text. The figure also shows the laboratory frame, and schematic illustrations of the substrate and derived orientation of the molecule with respect to the local electric fields defined by our experimental geometry. The reader is referred to the main text for more details.

References

[1] M. Fleischmann, P. J. Hendra, A. J. McQuillan, *Chem. Phys. Lett.*, 1974, **26**, 163.

[2] D. L. Jeanmaire and R. P. Van Duyne, *J. Electroanal. Chem.*, 1977, **84**, 1.

[3] M. Moskovits, *J. Chem. Phys.*, 1978, **69**, 4159.

[4] A. Otto, *Surf. Sci.*, 1978, **75**, L392.

[5] N. J. Halas, S. Lal, W. -S Chang, S. Link, P. Nordlander, *Chem. Rev.*, 2011, **111**, 3913.

[6] E. Hao, G. C. Schatz, *J. Chem. Phys.*, 2004, **120**, 357.

[7] F. J. Garcıa de Abajo, *J. Phys. Chem. C*, 2008, **112**, 17983.

[8] S. Nie, S. R. Emory, *Science*, 1997, **275**, 1102.

[9] K. Kneipp, Y. Wang, H. Kneipp, L. T. Perelman, I. Itzkan, R. R. Dasari, M. S. Feld, *Phys. Rev. Lett.*, 1997, **78**, 1667.

[10] E. C. Le Ru, P. G. Etchegoin, *Annu. Rev. Phys. Chem.*, 2012, **63**, 65.

[11] B. Pettinger, P. Schambach, C. J. Villagomez, N. Scott, *Annu. Rev. Phys. Chem.*, 2012, **63**, 379.

[12] M. Banik, A. Nag, P. Z. El-Khoury, A. Rodriguez-Perez, N. Guarrotxena, G. C. Bazan, V. A. Apkarian, *J. Phys. Chem. C*, 2012, **116**, 10415.

[13] M. Banik, P. Z. El-Khoury, A. Nag, A. Rodriguez-Perez, N. Guarrottxena, G. C. Bazan, V. A. Apkarian, *ACS Nano*, 2012, **6**, 10343.

[14] M. D. Sonntag, D. Chulhai, T. Seideman, L. Jensen, R. P. Van Duyne, *J. Am. Chem. Soc.*, 2013, **135**, 17187.

[15] P. Z. El-Khoury, W. P. Hess, *Chem. Phys. Lett.*, 2013, **581**, 57.

[16] P. Z. El-Khoury, D. Hu, W. P. Hess, *J. Phys. Chem. Lett.*, 2013, **4**, 3435.

[17] P. Z. El-Khoury, D. Hu, V. A. Apkarian, W. P. Hess, *Nano Lett.*, 2013, **13**, 1858.

[18] P. Z. El-Khoury, W. P. Hess, *Nano Lett.*, 2014, **14**, 4114.

[19] P. Z. El-Khoury, T. W. Ueltschi, A. L. Mifflin, D. Hu, W. P. Hess, *J. Phys. Chem. C*, 2014, **118**, 27525.

[20] P. Z. El-Khoury, Y. Gong, P. Abellan, B. W. Arey, A. G. Joly, D. Hu, J. E. Evans, N. D. Browning, W. P. Hess, *Nano Lett.*, 2015, DOI: 10.1021/acs.nanolett.5b00609

[21] R. Esteban, A. G. Borisov, P. Nordlander, J. Aizpurua, *Nat. Commun.*, 2012, **3**, 1.

[22] P. Z. El-Khoury, E. Khon, Y. Gong, A. G. Joly, P. Abellan, J. E. Evans, N. D. Browning, D. Hu, M. Zamkov, W. P. Hess, *J. Chem. Phys.*, 2014, **141**, 214308.

[23] A. Li, Z. Baird, S. Bag, D. Sarkar, A. Prabhath, T. Pradeep, R. G. Cooks, *Angew. Chem. Int. Ed.*, 2014, **53**, 12528.

[24] A. K. Badu-Tawiah , C. Wu, R. G. Cooks, *Anal. Chem.*, 2011, **83**, 2648.

[25] K. D. D. Gunaratne, V. Prabhakaran, Y. M. Ibrahim, R. V. Norheim, G. E. Johnson, J. Laskin, *Ann. Rev. Anal. Chem.*, 2011, **4**, 83.

[26] M. J. Frisch, G. W. Trucks, H. B. Schlegel *et al.*, GAUSSIAN 09, revision D.01 (Gaussian, Inc., Wallingford CT, 2009).

[27] A. D. Becke, *J. Chem. Phys.*, 1993, **98**, 5648.

[28] C. Lee, W. Yang, R. G. Parr, *Phys. Rev. B*, 1988, **37**, 785.

[29] S. H. Vosko, L. Wilk, M. Nusair, *Can. J. Phys.*, 1980, **58**, 1200.

[30] P. J. Stephens, F. J. Devlin, C. F. Chabalowski, M. J. Frisch, *J. Phys. Chem.*, **98**, 11623.

[31] R. Krishnan, J. S. Binkley, R. Seeger, J. A. Pople, *J. Chem. Phys.*, 1980, **72**, 650.

[32] A. D. McLean and G. S. Chandler, *J. Chem. Phys.*, 1980, **72**, 5639.

[33] K. Ruud, T. Helgaker, P. Bour, P., *J. Phys. Chem. A*, 2002, **106**, 7448.

[34] O. Quinet, B. Champagne, *J. Chem. Phys.*, 2001, **115**, 6293.

[35] V. Barone, *J. Chem. Phys.*, 2005, **122**, 014108.

[36] P. Z. El-Khoury, E. J. Bylaska, W. P. Hess, *J. Chem. Phys.*, 2013, **139**, 174303.

[37] P. Z. El-Khoury, K. Honkala, W. P. Hess, *J. Phys. Chem. A*, 2013, **118**, 8115.

[38] Z. Gao, J. P. Davies, M. J. Weaver, *J. Phys. Chem.*, 1990, **94**, 6858.

[39] P. Z. El-Khoury, S. J. Peppernick, D. Hu, Wayne P. Hess, *J. Phys. Chem. C*, 2013, **117**, 7260.